

Laminar-Turbulent Transition: The change of the flow state temperature with the Reynolds number

Sergei F. Chekmarev

Institute of Thermophysics, 630090 Novosibirsk, Russia, and

Department of Physics, Novosibirsk State University, 630090 Novosibirsk, Russia

(Dated: June 16, 2021)

Abstract

Using the previously developed model to describe laminar/turbulent states of a viscous fluid flow, which treats the flow as a collection of coherent structures of various size (Chekmarev, Chaos, 2013, 013144), the statistical temperature of the flow state is determined as a function of the Reynolds number. It is shown that at small Reynolds numbers, associated with laminar states, the temperature is positive, while at large Reynolds numbers, associated with turbulent states, it is negative. At intermediate Reynolds numbers, the temperature changes from positive to negative as the size of the coherent structures increases, similar to what was predicted by Onsager for a system of parallel point-vortices in an inviscid fluid. It is also shown that in the range of intermediate Reynolds numbers the temperature exhibits a power-law divergence characteristic of second-order phase transitions.

I. INTRODUCTION

In his famous work on statistical hydrodynamics [1], Onsager has predicted that a system of vortices can have negative temperature states, which can be interpreted as a clustering of vortices of the same sign. More specifically, Onsager considered a microcanonical ensemble of parallel point-vortices in an incompressible inviscid fluid confined to a finite region of physical space and calculated the entropy of the system S as a function of its energy E . Taking into account that the coordinates of point vortices obey Hamiltonian equations and thus are canonically conjugate, he concluded that the phase volume of the system $\Phi(E)$ is also finite, so that the density of states $\Gamma(E) = \Phi'(E)$ should have a maximum value at some (critical) energy E_m . Correspondingly, the statistical temperature $T = (dS/dE)^{-1}$, where $S(E) = \ln \Gamma(E)$ is the entropy, should be positive at $E < E_m$ and negative at $E > E_m$. Using these arguments, Onsager has concluded that "the large compound vortices formed in this manner will remain as the only conspicuous features of the motion; because the weaker vortices, free to roam practically at random, will yield rather erratic and disorganised contributions to the flow". This discovery of the negative temperature states has given rise to a number of theoretical considerations, where Onsager's arguments were revisited, discussed and elaborated [2–13] (for review, see Eyink and Sreenivasan [14] and Campa et al. [15]). In particular, it was shown that the key assumption of a finite region of physical space is not crucial because the accessible phase space is restricted by a constant of motion, which is an analog of enstrophy [6, 11].

Recently, we have proposed a statistical model for a fluid flow, which considers the flow as a collection of spatially localized (coherent) structures and uses the principle of maximum entropy to determine the most probable size distribution of the structures [16]. A principal difference of this model from the previous models in which a similar approach was used to describe inviscid flows (for a review of such models, see, e.g., Refs. 14 or 16) is that the structures are assumed to be composed of elementary cells in which the behavior of the particles (atoms or molecules) is uncorrelated. The characteristic size of elementary phase space volumes corresponding to these cells is determined by the kinematic viscosity of the fluid, which makes it possible to introduce the Reynolds number and thus to extend the statistical description of the flow to viscous fluids. The model successfully describes the transition to turbulence at large Reynolds numbers and some other characteristic properties

of turbulent flows [16]. Since the dependence of the energy and entropy of the flow on the Reynolds number is available in this model, the statistical temperature of the flow state can be calculated as a function the Reynolds number. In the present paper we show that at low Reynolds numbers, associated with laminar motion, the temperature is positive, and at high Reynolds numbers, associated with turbulent motion, it is negative. At intermediate Reynolds numbers, representing the transition range, the temperature changes from positive to negative as the structure size exceeds some critical value, similar to what was discovered by Onsager for the system of parallel point-vortices in a inviscid fluid. We also show that in the range of intermediate Reynolds numbers the temperature exhibits a power-law divergence characteristic of second-order phase transitions.

The paper is organized as follows. Section II briefly describes the statistical model of the flow that was developed in Ref. 16 and serves as an introduction to Sect. III. Section III introduces the statistical temperature of the flow states and presents the results of the study and their analysis, including the analogy with second-order phase transitions. Section IV contains concluding remarks.

II. THE MODEL

The model is briefly described as follows (for details, see Ref. [16]). Let a fluid flow be represented by a system of N identical particles (atoms or molecules) which are placed in a volume of physical space V . Assume that the particles can form spatially localized structures of N_i particles ($1 \leq N_i \leq N$), with the number of such (i) structures being M_i . These structures are viewed as coherent structures, i.e., the structures in which the constituting particles execute a concerted motion on the structure scale. Since such concerted motion should break down at the microscale level, each i structure can be divided into N_i/n elementary "cells" of volume v (each of n particles), in which the behavior of the particles is uncorrelated. Because the particles are identical, to each elementary cell there corresponds a 6-dimensional elementary volume of single-particle phase space, in which the state of the particles is uncertain. For a gas fluid, the velocity and linear scales of such a volume are, respectively, molecular thermal velocity c and mean free path λ (Kusukawa [17]). According to the kinetic theory of gases $c\lambda \sim \nu$, where ν is the kinematic viscosity (see, e.g., Ferziger and Kaper [18]), i.e., the characteristic linear size of the elementary phase volume is determined

by the kinematic viscosity [17]. For a liquid fluid, the linear size of the elementary volume can be taken to be $c^2\tau$, where c^2 is the fluctuation of the (molecular) kinetic energy per unit mass, and τ is the mean residence time of the molecule in a settled state, so that a similar estimate is valid, $c^2\tau \sim \nu$ (e.g., Frenkel [19]). Alternatively, the space and velocity scales of the volume can be associated with the corresponding Kolmogorov microscales [16], i.e., $\eta = (\nu^3/\epsilon)^{1/4}$ and $v_\eta = (\nu\epsilon)^{1/4}$, respectively (ϵ is the rate of dissipation per unit mass) [20, 21].

The given system of coherent structures is characterized by two parameters, which are the total number of particles (atoms or molecules) in the system N and the total energy E , i.e., the corresponding ensemble of the systems is a *microcanonical* ensemble. We assume that the total energy can be written as $E = \sum_i M_i E_i$, where E_i is the kinetic energy of the concerted motion of particles in i structure. This definition is based on two assumptions: i) the concerted motion of particles in each local region of the physical space is associated with one of the coherent structures and contributes to its kinetic energy, and ii) the potential energy of interaction of coherent structures is either negligible in comparison to the kinetic energy of the system or, if not, can be considered as a part of its kinetic energy, as, e.g., for the system of two-dimensional point vortices in inviscid fluid (Batchelor [22]), which was studied by Onsager [1]. Given the above definition of the total energy, the collection of the coherent structures can be treated as an ideal gas system, i.e., a system in which the potential energy is negligible and the total energy is additive (Landau and Lifshitz [23]). It is important that the ideal gas approximation does not imply that the interaction in the system is absent at all. One example, which was used by Ruelle [24] to draw an analogy to the turbulence cascade, is the heat conductivity in a rarefied gas: while the gas is considered to be an ideal gas, the heat transfer exists due to the energy exchange between the molecules in the course of their short-range collisions. This example is also useful in another respect. Although the process of the heat transfer is a non-equilibrium process, the molecular velocity distribution function, which corresponds to the the Fourier law, is just slightly different from the equilibrium (Maxwell) distribution, as a first-order perturbation of the latter (e.g., Ferziger and Kaper [18]). Therefore, if the statistical properties of the system is of interest, the equilibrium distribution function can be considered as a zero-order approximation.

Every distribution of particles (atoms or molecules) among the coherent structures that

satisfies the conditions $\sum_i N_i M_i = N$ and $E = \sum_i M_i E_i$ presents a *microstate* of the system at given N and E , and the number of such microstates $\Gamma(N, E)$ plays a role of the *density* of states. Taking into account that the particles are identical, so that the permutations of the particles in the elementary cells, the permutations of the elementary cells in the coherent structures, and the permutations of the coherent structures themselves do not lead to new states, we have

$$\Gamma(N, E) = \frac{N!}{\prod_i [(n!)^{N_i/n} (N_i/n)!]^{M_i} M_i!} \quad (1)$$

or, with the Stirling approximation $x! \approx (x/e)^x$ to be applicable

$$\Gamma(N, E) = \frac{(N/n)^N e^{N/n}}{\prod_i (N_i/n)^{N_i M_i/n} (M_i/e)^{M_i}} \quad (2)$$

Using Eq. (2), it is possible to calculate the most probable size distribution of the structures, $\tilde{M}_i = \tilde{M}_i(N_i)$, which maximizes the entropy $S(N, E) = \ln \Gamma(N, S)$ (the Boltzmann constant is set to unity) and determines the observational *macrostate* of the system. The variation of the entropy functional with respect to M_i at two conservation conditions $\sum_i M_i N_i = N$ and $\sum_i M_i E_i = E$ yields

$$\tilde{M}_i = \left(\frac{N_i}{n} \right)^{-\frac{N_i}{n}} e^{\alpha' N_i + \beta' E_i} \quad (3)$$

where α' and β' are the constants depending on N and E (the Lagrange multipliers).

To specify the dependence of E_i on N_i , we followed Kolmogorov [20], i.e., we assumed that the energy of concerted motion of particles increased with distance as $e(l) \sim l^{2h}$, where $h = 1/3$. Since the coherent structures may be different in form, the law of dependence of E_i on N_i can also be different. To estimate the law, we calculated the kinetic energy in a parallelepiped with sides L_1 , L_2 and L_3 as $E(L_1, L_2, L_3) \sim \int_{-L_1/2}^{L_1/2} \int_{-L_2/2}^{L_2/2} \int_{-L_3/2}^{L_3/2} r^{2h} dl_1 dl_2 dl_3$, where $r^2 = l_1^2 + l_2^2 + l_3^2$, and related the obtained energy to the parallelepiped volume $V = L_1 L_2 L_3$. The results of the calculations are presented in Fig. 1. Panel **a** shows typical coherent structures that were observed by Moisy and Jiménez in direct numerical simulations of isotropic turbulence [25], who characterized the structures by the aspect ratios L_1/L_2 and L_2/L_3 (solid triangles). There are also shown the corresponding structures we chosen to calculate the dependence of the kinetic energy on the structure volume (crosses). Panel **b** of Fig. 1 depicts the obtained dependence of E_i on V_i for these structures. As is seen, it is well fitted by the function $E \sim V^\gamma$ with $\gamma \approx 1.23$, which is close to $\gamma = 2h/3 + 1 = 11/9 \approx 1.22$ characteristic of the spherical structures [16]. The same exponent $\gamma = 11/9$ was used by

Ruelle [24], who, instead of introducing the coherent structures, divided the physical space in cubes in which the kinetic energy of fluctuations was assumed to obey the Kolmogorov theory [20]. In the present paper, the calculations are made with $\gamma = 11/9$. Assuming the density of the fluid to be constant, we thus have $E_i \sim N_i^\gamma$.

Strictly speaking, the Kolmogorov relation assumes the inertial interval of scales $\eta \ll l \ll L$, where η and L are the dissipation and external scales, respectively. However, for rough estimates, the range of its validity can be extended to the lower and upper bounds, i.e., to $\eta \leq l \leq L$ [16]. Moreover, with the arguments given by Landau and Lifshitz [21], the lower bound can be associated with laminar motion [16]. According to this, we associate the laminar state with the structures that are comparable in size with the elementary cell, i.e., $N_i/n \sim 1$, and the turbulent state with those that contain many elementary cells, i.e., $N_i/n \gg 1$.

After substituting the dependence E_i on N_i into Eq. (3), we eventually have

$$\tilde{M}_i = q_i^{-q_i} e^{\alpha q_i + \beta q_i^\gamma} \quad (4)$$

where $q_i = N_i/n$ is the number of the elementary cells in i structure, and α and β are new constants that should be determined from the equations of conservation of the total number of particles and kinetic energy in the form

$$N/n = \sum_i \tilde{M}_i q_i \quad (5)$$

and

$$E/n^\gamma = \sum_i \tilde{M}_i q_i^\gamma \quad (6)$$

It is also possible, and is more convenient, to vary α and β to obtain N/n and E/n^γ as functions of α and β [16].

The parameter N/n can be associated with the Reynolds number $\text{Re}_L = WL/\nu$, where W and L are, respectively, the velocity and linear scales characterizing the system as a whole. As has been mentioned, the characteristic size of the elementary phase volume is determined by the kinematic viscosity, so that the number of particles in the volume $n \sim \nu^3$. Correspondingly, the total number of particles N can be considered to be proportional to the total phase volume for the system, i.e., $N \sim (WL)^3$. Then $N/n \sim (WL/\nu)^3 = \text{Re}_L^3$, or assuming for simplicity that the coefficient of proportionality is equal to 1

$$\text{Re}_L = (N/n)^{1/3} \quad (7)$$

The distribution given by Eq. (4) is drastically different from the conventional Gibbs-Boltzmann distribution for a many-particle system (see, e.g., Landau and Lifshitz [23]). In particular, none of the Lagrange multipliers α and β can be associated with temperature. As has been shown in our previous paper [16], these multipliers determine the range of the Reynolds numbers where a turbulent state can be expected. To illustrate this, Fig. 2 shows the average number of elementary cells in the coherent structures $\langle q \rangle = \sum_i q_i \tilde{M}_i / \sum_i \tilde{M}_i$ as a function of the Reynolds number Re_L determined via Eqs. (5) and (7). The number of the elementary cells q_i varied from 1 to $q_{\max} = 200$; a variation of q_{\max} does not change the overall picture, except that the ranges of variation of $\langle q \rangle$ and Re_L extend to larger values of these quantities as q_{\max} increases [16]. The values of α and β were randomly chosen from the uniform distributions within $\alpha_{\min} \leq \alpha \leq \alpha_{\max}$ and $\beta_{\min} \leq \beta \leq \beta_{\max}$, respectively (for 10^5 samples in each case). As was indicated in Ref. 16, not every combination of α and β gives a physically reasonable bell-shaped distribution [26], i.e., for some combinations, the fraction of which is typically within several percentages, \tilde{M}_i does not vanish at $q \rightarrow q_{\max}$. In Fig. 2, the points with such "wrong" α/β combinations are excluded.

According to the present model, the points of Fig. 2 for which $\langle q \rangle \sim 1$ should be associated with a laminar state, and those for which $\langle q \rangle \gg 1$ with a turbulent state. A boundary that seemingly separates these states lies at a Reynolds number Re_L^* , which is between $\text{Re}_L \sim 10$ and $\text{Re}_L \sim 10^2$. The positions of the lower and upper boundaries of the manifold of points representing $\langle q \rangle$ as a function of Re_L are determined by the maximum values of β and α , respectively [16]. The lower boundary shifts to lower values of Re_L as β increases, and the upper boundary shifts to larger values of Re_L as α increases, specifically as $\text{Re}_L \sim \exp(-0.15\beta\langle q \rangle)$ and $\text{Re}_L \sim \exp(0.06\alpha\langle q \rangle)$, respectively. However, while the upper boundary shifts unlimitedly, the lower boundary changes its position until the value $\beta \approx 1.5$ is reached, after that it "freezes" [16] (see also Fig. 2). It is significant that the dependence of $\langle q \rangle$ on Re_L is not unique, i.e., the state of the flow is not solely determined by the Reynolds number; rather, as is well-known, it can depend on the type of the flow, the inlet conditions, the flow environment, etc. [27]. In this respect, it is important that for large values of α , the states with $\langle q \rangle \sim 1$ are present at the Reynolds numbers far above its "critical" value Re_L^* ; for example, at $\alpha = 50$ the values of $\langle q \rangle \approx 3$ are found up to $\text{Re}_L \sim 1 \times 10^4$. The model thus predicts that the flow should not only be laminar at $\text{Re}_L < \text{Re}_L^*$ but can also remain laminar at $\text{Re}_L \gg \text{Re}_L^*$, as it was observed, e.g., for pipe flows by Reynolds [28]

and confirmed in many subsequent studies [29–31]. We note that the specific properties of the coherent structures, i.e., the structure shape and the velocity distribution inside the structure, do not seem to be of critical importance here. In particular, the structures in the form of the Burgers vortices of finite length (to mimic "worms") lead to the dependence of the structure size on the Reynolds number that is qualitatively similar to that in Fig. 2 [16].

A highly nontrivial property of the present system, which distinguishes it from the conventional many-particle systems in statistical physics [23], is that the entropy of the system is non-additive. For example, if we divide the given system of N particles into k identical and noninteracting subsystems, the density states of the composite system will be

$$\Gamma_{\Sigma} = \frac{[(N/k)!]^k}{\{\prod_i [(n!)^{N_i/n} (N_i/n)!]^{L_i} L_i!\}^k} \quad (8)$$

where $L_i = M_i/k$. Comparison of this equation with Eq. (1) yields

$$S_{\Sigma} - S = \ln(\Gamma_{\Sigma}/\Gamma) = \sum_i (1 - N_i) M_i \ln k \approx -N \ln k = -n \text{Re}_L^3 \ln k < 0 \quad (9)$$

where S_{Σ} and S are the entropies of the composite and original systems, respectively. The non-additivity of entropy is consistent with the fact that the system of particles representing a fluid flow cannot be divided into parts without a loss of its essential properties. According to Eq. (7), the division of the system into subsystems will reduce the Reynolds number characterizing a subsystem (in the above example, in $k^{1/3}$ times), so that the resulting Reynolds number for the subsystem will not correspond to the flow state in the subsystem, which is assumed to be the same as in the total system. In other words, the condition that the Reynolds number is determined by the number of particles in the system [Eq. (7)], originates a virtual interaction of the coherent structures that makes unfavorable the separation of the flow into domains at equilibrium. As can be seen from Eq. (1), the entropy of the system is additive only at the level of the coherent structures, i.e., each collection of the structures of a specific size gives an additive contribution to the system entropy.

According to Eq. (1), the density of states Γ and, correspondingly, the entropy $S = \ln \Gamma$, assume that the particles (atoms or molecules) are identical, and an elementary volume of the phase space exists in which the state of the particles is uncertain. The same assumptions play a key role in the derivation of the Navier-Stokes equation from the the Liouville equation, and thus they are implicitly present in the Navier-Stokes equation [16] (for the procedure of the derivation of the Navier-Stokes equation for a gas fluid from the Liouville equation see, e.g.,

Ferziger and Kaper [18]). More specifically, assuming the particles to be identical (the first assumption of the present model), the Liouville equation for the many-particle distribution function is reduced to a kinetic equation which contains single-particle and two-particle distribution functions (the Bogoliubov-Born-Green-Kirkwood-Yvon hierarchy). Then, using the molecular chaos assumption (which corresponds to the second assumption of the model), this equation is closed by expressing the two-particle distribution function through the single-particle one to yield the Boltzmann equation. The Navier-Stokes equation is obtained from the Boltzmann equation in the limit of small Knudsen number $\text{Kn} = \lambda/L$, as the first-order correction in Kn to the Euler equation, which describes the gas motion in a state of local equilibrium (the Chapman-Enskog expansion). Therefore, although the Navier-Stokes equation is incomparably rich in the description of the laminar/turbulent transition, giving a dynamic picture of the process, it is reasonable to expect that the statistical properties of the flow calculated on the basis of the Navier-Stokes equation are, in a considerable degree, due to the above assumptions involved in the derivation of the Navier-Stokes equation (they can be considered as a hidden statistical content of the Navier-Stokes equation).

III. TEMPERATURES OF THE FLOW STATES: RESULTS AND DISCUSSION

Following Onsager [1], let us consider local temperatures of flow states, which in our case will be related to the coherent structures of different size

$$1/T_i = \Delta S_i^{\text{cum}} / \Delta E_i^{\text{cum}} \quad (10)$$

where $E_i^{\text{cum}} = \sum_1^i E_k$ and $S_i^{\text{cum}} = \sum_1^i S_k$ are the "cumulative" distributions of the energy and entropy, respectively, and the increment is calculated as $\Delta X_i = X_i - X_{i-1}$. The quantities E_i^{cum} and S_i^{cum} play a role of the energy E and entropy S in the Onsager theory [1]. In particular, the energies are similar in two important respects. First, E_i^{cum} increases as the coherent structures of larger size are included into consideration, similar as E increased because of clustering of vortices of the same size in the Onsager theory. Secondly, since the Hamiltonian for the system of two-dimensional point vortices in inviscid fluid is the part of the kinetic energy of the system that depends on the relative positions of the vortices (Batchelor [22]), the total energy E considered by Onsager represents the kinetic energy, i.e., similar to what we assumed for the total energy of the system of coherent structures

(Sect. II). The difference with the Onsager theory is that in our case, because we consider a viscous fluid, the temperature distribution also depends on the Reynolds number Re_L as on a parameter. Taking into account Eqs. (2), (4) and (6), we have

$$E_i^{\text{cum}} = A \sum_{k=1}^{k=i} \tilde{M}_k q_k^\gamma \quad (11)$$

and

$$S_i^{\text{cum}} = \ln \Gamma_i^{\text{cum}} = - \sum_{k=1}^{k=i} \tilde{M}_k (q_k \ln q_k + \ln \tilde{M}_k - 1) + B \quad (12)$$

where $A = n^\gamma$ and $B = N \ln(N/n) + N/n$. Then, assuming N and n to be fixed, so that the Reynolds number determined by Eq. (7) is fixed too, Eq. (10) gives

$$\frac{1}{T_i} = - \frac{\tilde{M}_i (q_i \ln q_i + \ln \tilde{M}_i - 1)}{A \tilde{M}_i q_i^\gamma} = - \frac{\alpha q_i + \beta q_i^\gamma - 1}{A q_i^\gamma} \quad (13)$$

To represent the temperature in the subsequent Figs. 3-5, the constant A is set to unity.

Examination of the temperature distributions given by Eq. (13) shows that they are characteristically different in different ranges of variation of the Reynolds number. Specifically, the distributions of three types are observed, which are depicted in Fig. 3. At small Re_L the temperature is positive for all q_i (the red curve), at large Re_L it is negative for all q_i (the blue curve), and at intermediate values of Re_L , the temperature abruptly changes from positive to negative at some $q_i = q_i^c$, which corresponds to the maximum of the entropy (the black curve). In the latter case, the behavior of the temperature is qualitatively similar to what was predicted by Onsager [1]. The essential difference is that in the present case the distribution is dependent upon the Reynolds number as on a parameter; in particular, the value of q_i^c changes with Re_L , although not regularly because different combinations of parameters α and β entering Eq. (13) can lead to very close values of Re_L (as, e.g., Fig. 2 evidences).

To see how the temperature of state changes with the Reynolds number, let us introduce average temperatures $\langle T \rangle$ which are characteristic of different Re_L . If the temperature is positive or negative for all q_i , as for $\text{Re}_L \ll \text{Re}_L^*$ and $\text{Re}_L \gg \text{Re}_L^*$ in Fig. 3, it was calculated as an overall average $\langle T \rangle = \sum_i T_i \tilde{M}_i / \sum_i \tilde{M}_i$, where \tilde{M}_i is the most probably size distribution of the structures, Eq. (4). Otherwise, if the sign of the temperature changes, as for $\text{Re}_L \sim \text{Re}_L^*$ in Fig. 3, it was calculated for the $T_i > 0$ and $T_i < 0$ segments of the dependence $T_i = T_i(q_i)$ separately. The results of the calculations are presented in Fig. 4. It is seen that the overall

average temperature drastically diverges, changing from positive to negative as the Reynolds number increases. This divergence of the overall average temperature is accompanied by large fluctuations of the segment average temperatures in a relatively wide range of the Reynolds numbers. The state of the flow that has the temperature of the same sign for all coherent structures, i.e., the overall average temperature, should be associated with a certain state of the flow, which is laminar or turbulent. Therefore, the laminar and turbulent states, which correspond to small and large Reynolds numbers, are characterized by positive and negative temperatures, respectively. Correspondingly, the range of the Reynolds numbers where the positive and negative temperatures are in mixture should be associated with the laminar-turbulent transition range.

Figure 4 suggests that the laminar-turbulent transition is similar to a second-order phase transition [23] in that at some critical Reynolds number the temperature drastically diverges, which is accompanied by large fluctuations of the temperature. A similarity between these two phenomena has been noticed and discussed in Refs. 33–35, where laminar-turbulent transition was studied experimentally. Chabaud et al. [33] investigated a jet of gaseous helium and found that in the transition range the behavior of the width of the velocity probability density function depending on the size of the spatial structures resembled the isotherms of a liquid-gas system near the critical point. Tabeling and Willaime [34] studied the flatness of the velocity derivatives in the flow of gaseous helium between counter-rotating disks (a von Kármán swirling flow) and showed that in the transition range the flatness experiences significant changes and has a power-law dependence on the Reynolds number as $\sim \text{Re}^{0.54}$ below the critical number Re_c and $\sim (\text{Re} - \text{Re}_c)^{0.5}$ above Re_c . More recently, Cortet et al. [35] investigated the susceptibility of the von Kármán swirling liquid water flows to symmetry breaking initiated by different rotation frequencies of the disks and found that at a critical Reynolds number Re_c the susceptibility diverges as $\chi_1 \sim |1/\log \text{Re} - 1/\log \text{Re}_c|^{-1}$. The quantity $1/\log \text{Re}$ was interpreted as a temperature due to Castaing [36], who introduced the turbulent flow temperature as a quantity that is conserved along the length scales in the energy cascade.

The present model shows a similar qualitative behavior of the state temperature as a function of the Reynolds number Re_L . To determine critical exponents, we averaged the data of Fig. 4 by dividing the Reynolds numbers into bins of length 0.1 (all temperatures were taken into account, not only those shown in Fig. 4). In each bin, the mean values of the

Reynolds number (R) and the temperature (Θ) were calculated. The obtained dependence of Θ on R was fitted to the function $\Theta_{\text{theor}} = a|R - \text{Re}_L^*|^b$ separately for $R < \text{Re}_L^*$ and $R > \text{Re}_L^*$, where a and b are the constants to be fitted, and Re_L^* is an expected critical Reynolds number (Fig. 5). The constant b plays a role of the critical exponent. To determine constants a and b for a selected value of Re_L^* , the functional $Q = \sum[(\Theta_i - \Theta_{\text{theor},i})/\sigma_i]^2$ was evaluated, where i is the number of the bin, and σ_i is the standard deviation of Θ_i in i bin. The functional was minimized with respect to a and b in a close vicinity of Re_L^* ($|R - \text{Re}_L^*| \leq 0.5$). To find an optimal value of Re_L^* , the procedure was repeated for different values of Re_L^* that increased from 1.5 to 1.9. The value of Re_L^* was considered to be optimal if the both final values of Q for $R < \text{Re}_L^*$ and $R > \text{Re}_L^*$ were smaller than the corresponding values of Q for the other values of Re_L^* . The best fit was achieved at $\text{Re}_L^* = 1.578$, in which case the data are approximated by the functions $\Theta = 0.42(\text{Re}_L^* - R)^{-1.42}$ at $R < \text{Re}_L^*$ and $\Theta = -2.2(R - \text{Re}_L^*)^{-1.42}$ at $R > \text{Re}_L^*$ (Fig. 5). The fluctuations of the temperature sharply increase toward the critical Reynolds number (exponentially rather than by a power law) and reach $\sigma/\Theta \sim 1$ and $\sigma/\Theta \sim 10$ at $R < \text{Re}_L^*$ and $R > \text{Re}_L^*$, respectively.

The observed behavior of the temperature with the Reynolds number is similar to second-order phase transitions in several essential respects: the temperature exhibits a power-law divergence at the critical point (the critical Reynolds number), the critical exponents below and above the critical point are practically equal to each other and have the same order of magnitude as those in second-order phase transitions, and the fluctuations of the temperature in the vicinity of the critical point are as large or larger than the mean value of the temperature (Stanley [37]). At the same time, drawing a direct analogy to second-order phase transitions is problematic, primarily because the flow cannot be divided into parts without a loss of its essential properties (Sect. II). Consequently, the system of particles representing the flow does not have the property of self-similarity, which plays a key role in second-order phase transitions and critical phenomena (Kadanoff [38] and Wilson [39]).

The drastic change of the state temperature at $\text{Re}_L \sim \text{Re}_L^*$ offers a criterion to distinguish between laminar and turbulent states that is more definite than the dependence of $\langle q \rangle$ upon Re_L (Fig. 2). The unreasonably low value of Re_L^* (≈ 1.6) we obtained is, in a considerable degree, a result of the flexibility in the definition of the size of the elementary volume. Equation (7) assumed that it was the product of the Kolmogorov length and velocity dissipation microscales $\eta v_\eta = \nu$. However, the space scale must not be necessarily equal to

η . For example, the scale dividing the dissipation and inertial subranges $l_{\text{DI}} = 60\eta$ (Pope [40]) can be taken as the space scale. Correspondingly, because in the inertial subrange $v \sim (\epsilon l)^{1/3}$, $v_{\text{DI}} = (\epsilon l_{\text{DI}})^{1/3}$ can serve as the velocity scale. Then, the value of the critical Reynolds number Re_L^* increases $60^{4/3}$ times, which leads to a more reasonable value of $\text{Re}_L^* \approx 4 \times 10^2$.

It would be of interest to determine the statistical temperature of the flow by experiment or numerical simulations and test the predicted behavior of the temperature with the Reynolds number. For this, Eq. (13) can be rewritten as $1/T_i \sim -(q_i \ln q_i + \ln M_i - 1)/E_i$, where E_i is the kinetic energy of i structure, M_i is the size distribution of the structures, and $q_i = V_i/\eta^3$, where V_i is the volume of i structure, and η is the Kolmogorov microscale. According to this equation, all one needs to know to calculate the temperature is the volumes of the coherent structures, their kinetic energies, and the size distribution of the structures. Such information can be obtained, in principle, by direct numerical simulations, similar to those of Moisy and Jiménez [25], in which the size distribution of the coherent structures was determined and the kinetic energies of the structures could be calculated. of the structures could be calculated.

IV. CONCLUSIONS

Using the previously developed statistical model of laminar/turbulent states of a fluid flow, which considered the flow as a collection of coherent structures of various size [16], a statistical temperature of the flow states has been determined that depends on the Reynolds number. It has been shown that at small Reynolds numbers, associated with laminar states, the temperature is positive, while at large Reynolds numbers, associated with turbulent states, it is negative. At intermediate Reynolds numbers, the temperature abruptly changes from positive to negative as the structure size increases, similar to what Onsager predicted for a system of parallel point-vortices in an inviscid fluid [1]. It has also been shown that in the range of intermediate Reynolds numbers, which is associated with the transition between laminar and turbulent states, the temperature drastically diverges, exhibiting a power-law behavior characteristic of second-order phase transitions. The critical exponents below and above critical Reynolds number are close to each other and have the same order of magnitude as those in the second-order phase transitions.

V. ACKNOWLEDGMENTS

I thank R. Khairulin for useful discussions of the critical phenomena.

-
- [1] L. Onsager, *Nuovo Cimento Suppl.* **6**, 279 (1949).
 - [2] G. Joyce and D. Montgomery, *J. Plasma Phys.* **10**, 107 (1973).
 - [3] S. F. Edwards and J. B. Taylor, *Proc. R. Soc. Lond. A* **336**, 257 (1974).
 - [4] D. Montgomery and G. Joyce, *Phys. Fluids* **17**, 1139 (1974).
 - [5] Y. B. Pointin and T. S. Lundgren, *Phys. Fluids* **19**, 1459 (1976).
 - [6] T. S. Lundgren and Y. B. Pointin, *J. Stat. Phys.* **17**, 323 (1977).
 - [7] R. H. Kraichnan and D. Montgomery, *Rep. Prog. Phys.* **43**, 547 (1980).
 - [8] J. Fröhlich and D. Ruelle, *Commun. Math. Phys.* **87**, 1 (1982).
 - [9] J. Miller, *Phys. Rev. Lett.* **65**, 2137 (1990).
 - [10] A. J. Chorin, *Commun. Math. Phys.* **141**, 619 (1991).
 - [11] G. L. Eyink and H. Spohn, *J. Stat. Phys.* **70**, 833 (1993).
 - [12] S. Jung, P. J. Morrison, and H. L. Swinney, *J. Fluid Mech.* **554**, 433 (2006).
 - [13] P.-H. Chavanis, *Eur. Phys. J. Plus* **127**, 159 (2012).
 - [14] G. L. Eyink and K. R. Sreenivasan, *Rev. Mod. Phys.* **78**, 87 (2006).
 - [15] A. Campa, T. Dauxois, S. Ruffo, *Phys. Rep.* **480**, 57 (2009).
 - [16] S. F. Chekmarev, *Chaos* **23**, 013144 (2013).
 - [17] K. Kusukawa, *J. Phys. Soc. Jap.* **6**, 86 (1951).
 - [18] J. H. Ferziger and H. G. Kaper, *Mathematical Theory of Transport Processes in Gases* (North-Holland, Amsterdam, 1972).
 - [19] J. Frenkel, *Kinetic Theory of Liquids* (Dover, New York, 1955).
 - [20] A. N. Kolmogorov, *Dokl. Akad. Nauk SSSR* **30**, 301 (1941); reprinted in *Proc. R. Soc. Lond. A* **434**, 9 (1991).
 - [21] L. D. Landau and E. M. Lifshitz, *Fluid Mechanics* (Pergamon, New York, 1987).
 - [22] G. K. Batchelor, *An Introduction to Fluid Dynamics* (Cambridge Univ. Press, 1970).
 - [23] L. D. Landau and E. M. Lifshitz, *Statistical Physics* (Pergamon, New York, 1980).
 - [24] D. P. Ruelle, *Proc. Natl. Acad. Sci. USA* **109**, 20344 (2012).

- [25] F. Moisy and J. Jiménez, *J. Fluid Mech.* **513**, 111 (2004).
- [26] J. Jiménez, A. A. Wray, P. G. Saffman, and R. S. Rogallo, *J. Fluid Mech.* **255**, 65 (1993).
- [27] M. Lesieur, *Turbulence in Fluids* (Springer, Dordrecht, 2008).
- [28] O. Reynolds, *Phil. Trans. R. Soc. Lond. A* **174**, 935 (1883).
- [29] W. Pfenninger, in *Boundary Layer and Flow Control*, edited by G. V. Lachman (Pergamon, Oxford, 1961) p. 961.
- [30] A. G. Darbyshire and T. Mullin, *J. Fluid Mech.* **289**, 83 (1995).
- [31] B. Eckhardt, T. M. Schneider, B. Hof and J. Westerweel, *Annu. Rev. Fluid Mech.* **39**, 447 (2007).
- [32] U. Frisch, *Turbulence: The Legacy of A. N. Kolmogorov* (Cambridge Univ. Press, 1995), p. 244.
- [33] B. Chabaud, A. Naert, J. Peinke, F. Chillà, B. Castaing, and B. Hébral, *Phys. Rev. Lett.* **73**, 3227 (1994).
- [34] P. Tabeling and H. Willaime, *Phys. Rev. E* **65**, 066301 (2002).
- [35] P.-P. Cortet, A. Chiffaudel, F. Daviaud, and B. Dubrulle, *Phys. Rev. Lett.* **105**, 214501 (2010).
- [36] B. Castaing, *J. Phys. II (France)* **6**, 105 (1996).
- [37] H. E. Stanley, *Introduction to Phase Transitions and Critical Phenomena* (Oxford University Press, Oxford and New York, 1971).
- [38] L. P. Kadanoff, *Physics* **2**, 263 (1966).
- [39] K.G. Wilson, *Rev. Mod. Phys.* **47**, 773 (1975).
- [40] S. B. Pope, *Turbulent Flows* (Cambridge Univ. Press, 2000).

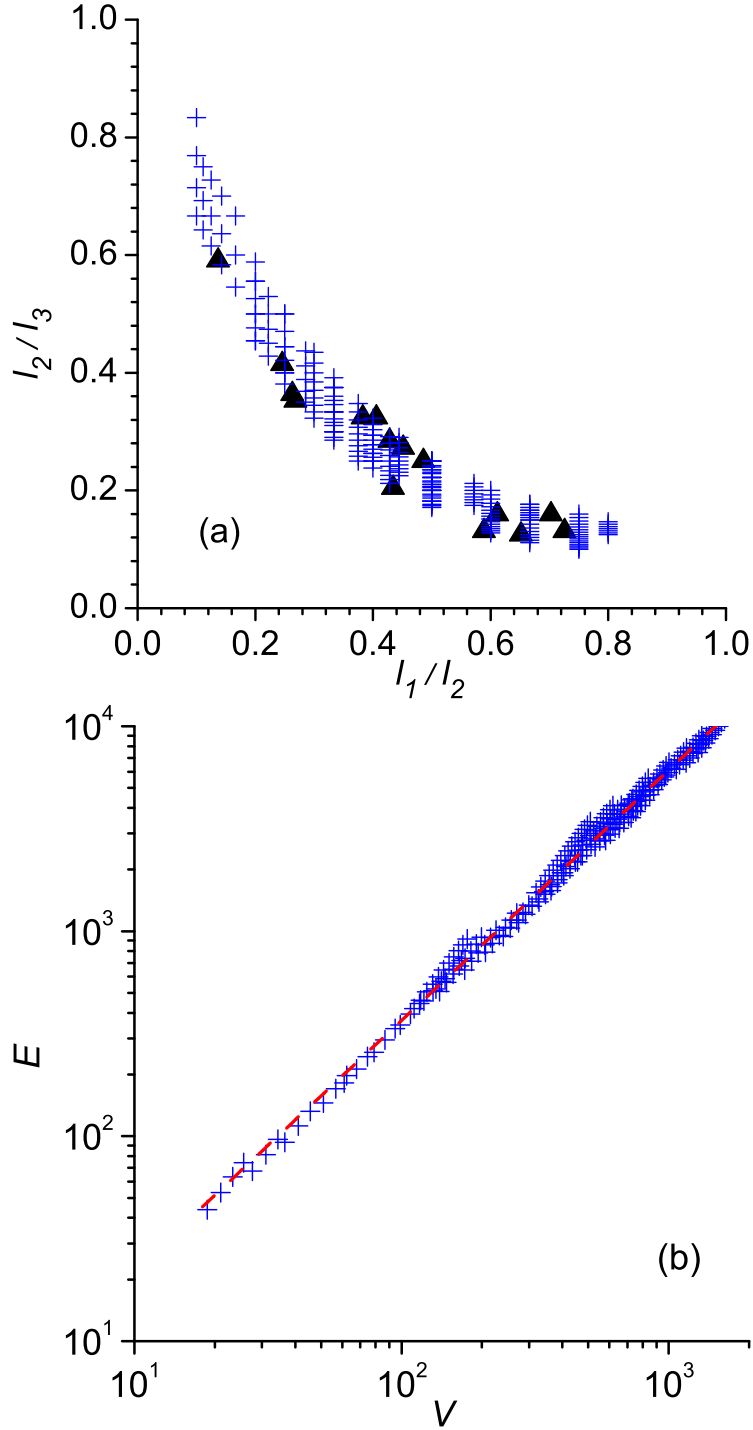


FIG. 1: (Color online) Properties of the coherent structures. (a) The aspect ratios of the structures: the triangles correspond to Ref. 25, and the crosses to the present work. (b) The kinetic energy of the structure versus its volume: the crosses correspond to points shown by crosses in panel (a), and the dashed line shows the fitting of the data to the power function $E \sim V^{1.23}$.

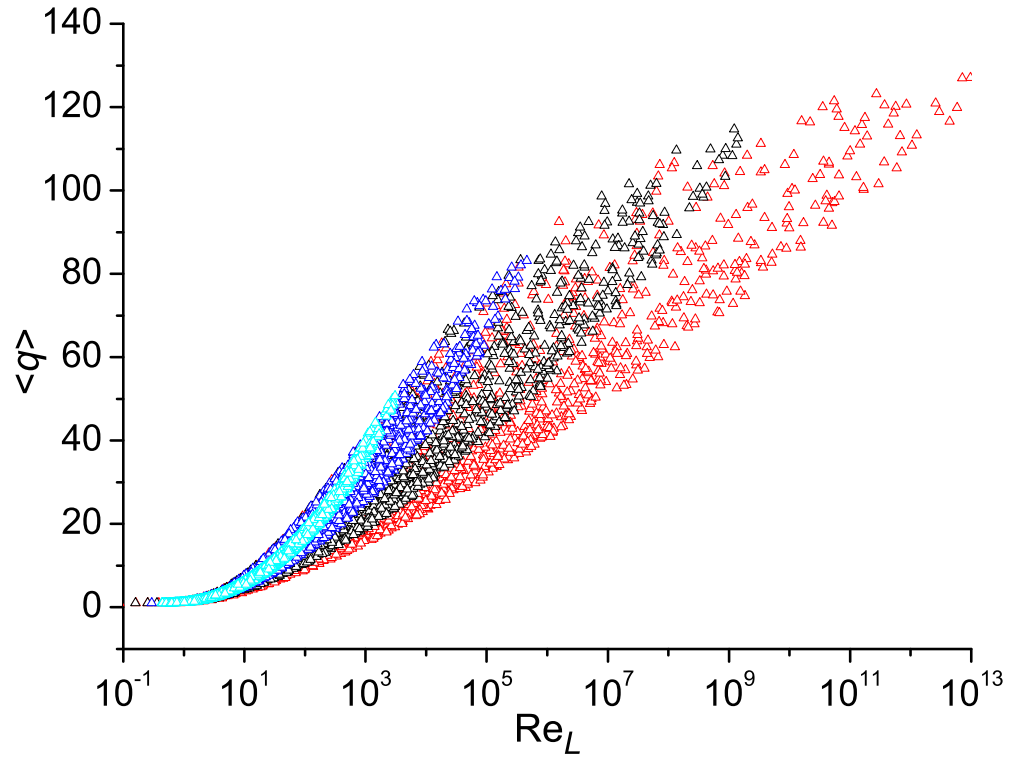


FIG. 2: (Color online) Average number of the elementary cells in the coherent structures as a function of the Reynolds number. The constants α and β vary from -1.3 to 1.3 (cyan labels), -2.0 to 2.0 (blue), -3.0 to 3.0 (black), and -4.0 to 4.0 (red).

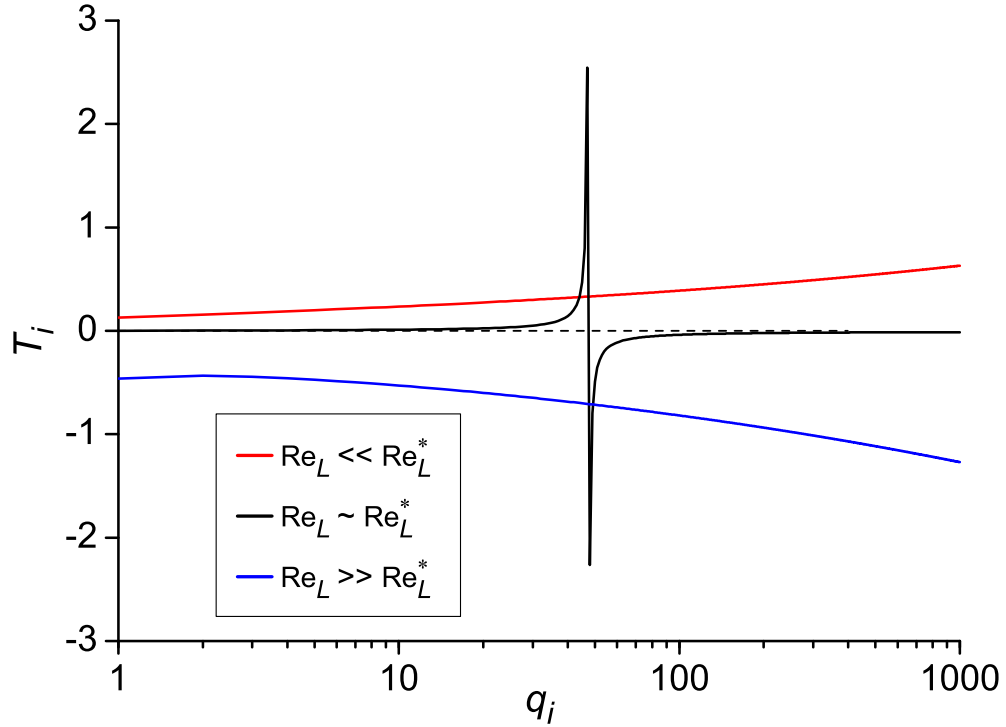


FIG. 3: (Color online) Characteristic dependencies of the flow state temperature on the structure size. The red, black and blue curves are for the small, intermediate and large Reynolds numbers, respectively. Specifically, the curves correspond to $Re_L = 0.2$ (red), $Re_L = 1$ (black), and $Re_L = 100$ (blue). For illustration purpose, the temperature given by the black curve is decreased by 50 times.

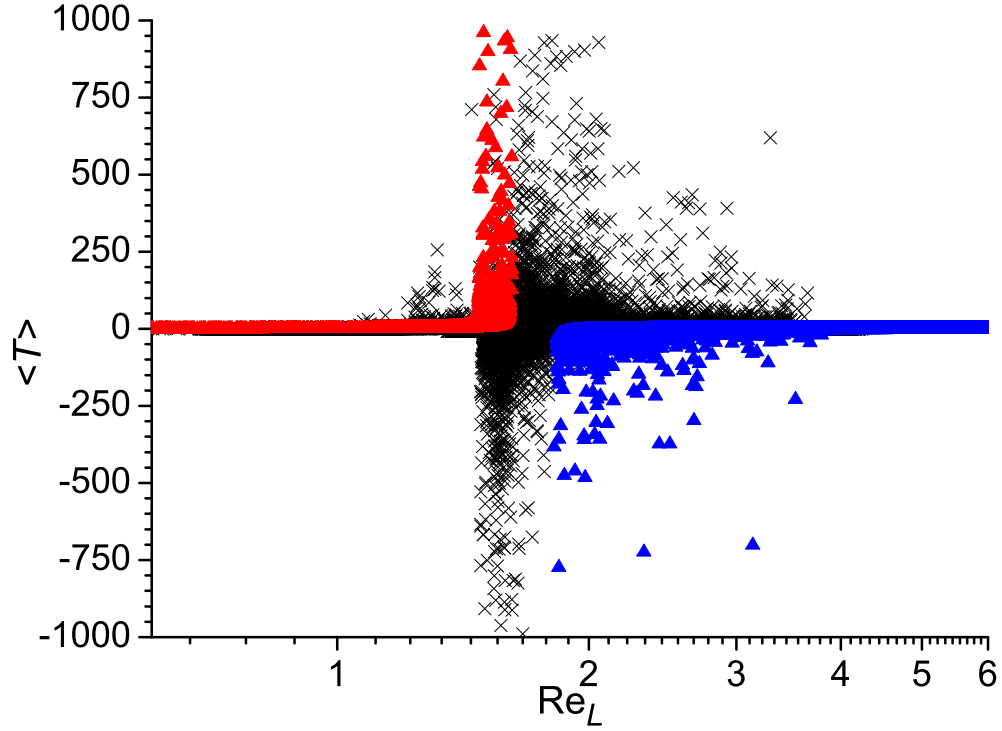


FIG. 4: (Color online) Average temperatures of the flow states as a function of the Reynolds number. The red triangles correspond to the laminar state, the blue triangles to the turbulent state, and the crosses to the transition states. To generate the values of T_i to be averaged, the constants α and β varied from -7.0 to 7.0 . For purpose of illustration, not all points are shown: the temperatures are restricted by the value of $|\langle T \rangle| = 10^3$ (though they can be as large as $|\langle T \rangle| \sim 10^4$), and only the points whose weight in each subset of the points (represented by the red and blue triangles, and the crosses) are not less than 1×10^{-6} .

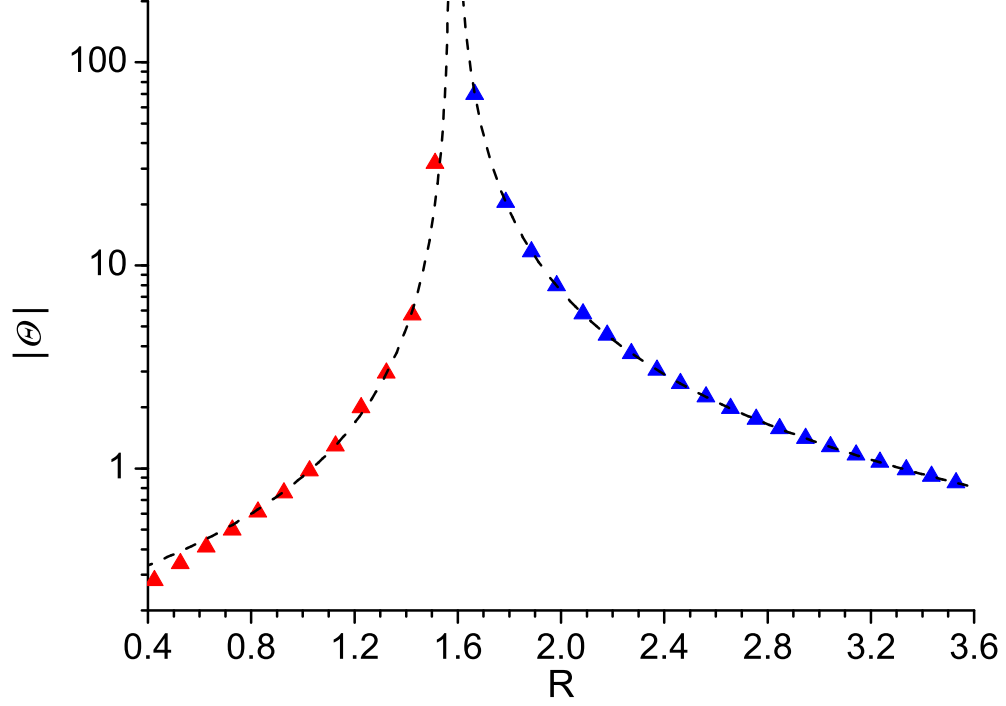


FIG. 5: (Color online) Critical behavior of the statistical temperature. The data of Fig. 4 are averaged for the Reynolds number intervals $\Delta\text{Re}_L = 0.1$. The red triangles correspond to the states below Re_L^* , and the blue triangles to the states above Re_L^* ($\text{Re}_L^* = 1.578$). The dashed curves show the best fits to the power functions $\Theta = 0.42(\text{Re}_L^* - R)^{-1.42}$ (the red triangles) and $\Theta = -2.2(R - \text{Re}_L^*)^{-1.42}$ (the blue triangles).